PERFORMANCE OF SMART ANTENNA ARRAYS WITH MAXIMAL-RATIO EIGEN-COMBINING

Constantin Siriteanu and Steven D. Blostein
Department of Electrical and Computer Engineering
Queen's University, Kingston, Ontario, K7L3N6, Canada
email: costi@ee.queensu.ca, sdb@ee.queensu.ca

Abstract

Conventionally, maximum average signal-to-noise ratio beamforming (Max-ASNR BF) and maximal-ratio combining (MRC) are applied to antenna array systems. A recently-proposed combining approach based on the Karhunen-Loève Transform (KLT) followed by MRC of the strongest resultant signals, denoted herein as maximal-ratio eigen-beamforming (MREC), was claimed to be superior and flexible compared to Max-ASNR BF and MRC for correlated, imperfectly-estimated channels, but comprehensive analytical tools required to understand, evaluate and apply MREC to smart antenna arrays were not available. For Rayleigh fading and BPSK modulation, general MREC average error probability (AEP) expressions are derived herein for correlated channels which are imperfectly estimated. Particular cases of these formulas also describe Max-ASNR BF and MRC of the original untransformed received signals (MRCO). A criterion which allows flexible MREC tuning to the actual environment by trading-off detection performance versus complexity is proposed. The analytical results are applied for channel estimation using pilot-symbol-aided modulation (PSAM) and interpolation and they show that significant gains can be obtained with MREC-based smart antenna arrays in scenarios with significant correlation of the received signals, compared to Max-ASNR BF as well as MRCO.

Index Terms

Beamforming, BPSK modulation, correlated channels, diversity, imperfect channel estimates, maximal-ratio eigen-combining, Rayleigh fading.

I. INTRODUCTION

Antenna arrays enhance the capabilities (capacity, range, data rate) of wireless communication links by combating fading and by boosting the intended signal relative to noise and interference.

In a wireless link, spatial fading may occur because multiple replicas of the transmitted signal may arrive at the receiver from many distinct angles. The azimuthal angle of arrival (AOA) of these paths is a random variable whose distribution depends on scattering. The AOA standard deviation is generally denoted as *angle spread* [1].

The angle spread directly impacts the correlation of the signals received at an antenna array [1] [2] [3]: large angle spread induces low correlation and vice-versa. For perfectly-known channels and no interference (this latter assumption holds throughout this work), maximal-ratio combining [4] (MRC) is optimum regardless of the combined signals' correlations. However, MRC yields lowest average probability of error (AEP) for uncorrelated channels. On the other hand, maximum average signal-to-noise ratio beamforming [5] (Max-ASNR BF) yields lowest AEP when the signals are completely correlated (coherent). Naturally then, Max-ASNR BF is conventionally proposed for scenarios with line-of-sight and/or negligible angle spread, while MRC is employed otherwise.

Max-ASNR BF relies on the covariance of the channel vector, which, compared to the channel coherence time, is considered a long-term channel feature since averaging is performed over temporal fading and noise [3] [6]. Max-ASNR BF has low complexity and offers antenna gain but no diversity gain [2] [7]. On the other hand, MRC exploits only short-term channel features since averaging is over noise only. MRC offers maximum diversity gain, but its performance may be impaired by poor and computationally-intensive short-term channel estimation [6]. Obviously, applying these well-established combining techniques may be somewhat rigid in practice since the angle spread may also change over time.

The pitfalls of Max-ASNR BF and MRC lead to the development of the so-called *eigen-beamforming* [3], which we refer to as maximal-ratio eigen-combining (MREC) herein. In MREC, appropriately-chosen eigenvectors of the covariance of the channel vector form the Karhunen-Loève Transform (KLT) of the received signal vector. The strongest resultant signals are then combined using the MRC criterion.

Several authors have claimed mainly based on simulation results that MREC has better symbol-detection performance than Max-ASNR BF in scenarios with angle spread [6] [7] [8],

since MREC takes advantage of available diversity gain. MREC was also shown [6] [9] to outperform MRC on the original untransformed signal vector (denoted further as MRCO) in scenarios with correlated received signals and imperfect channel estimation, as MREC may reduce the dimension of the short-term processing problem and produce improved short-term estimates [3] [6]. However, the previously-proposed MREC analysis [9] and tuning method [10] have applicability limited to certain channel estimation methods.

Therefore, in this paper we analyze MREC to find more general AEP-expressions and method for adaptive tuning. Based on analysis results we compare MREC with Max-ASNR BF and MRCO from the detection performance standpoint.

This work is organized as follows: we first present the signal model and the MREC approach for perfect channel knowledge. We then briefly describe the pilot-symbol-aided modulation (PSAM) technique which can be exploited using interpolation for channel estimation. In Section III we describe an approximate MREC (AMREC) approach which is widely used when the channel is estimated, and, for Rayleigh fading and BPSK signals, we obtain a novel and general AEP-expression required for a study of a AMREC-based antenna array employed in environments with angle spread. Special cases apply to Max-ASNR BF, and approximate MRCO (AMRCO) for data-independent interpolation. In Section IV we analyze the less-known exact MREC (EMREC) approach, and based on its AEP-formula we devise in Section V a criterion which trades-off detection performance versus complexity and adaptively tunes a MREC-based antenna to the actual environment. In Section VI we provide numerical results for the AEP of MREC, Max-ASNR BF and MRCO as applied to a uniform linear antenna array (ULA). These results show that significant benefits in terms of detection performance and flexibility are possible by employing MREC with adaptive tuning based on the proposed criterion in scenarios with high correlation among received signals.

II. MAXIMAL-RATIO EIGEN-COMBINING (MREC)

Consider that L copies of a BPSK signal affected by Rayleigh fading and zero-mean additive noise are available for processing at the receiver. After demodulation, matched-filtering and symbol-rate sampling, the complex-valued received signal vector can be written as:

$$\tilde{\mathbf{y}} = \sqrt{E_b}\; b\; \tilde{\mathbf{h}} + \tilde{\mathbf{n}} \tag{1}$$

where E_b is the energy transmitted per symbol, $b \in \{\pm 1\}$ is the equiprobable binary random symbol, $\tilde{\mathbf{h}}$ and $\tilde{\mathbf{n}}$ are the complex zero-mean Gaussian channel and noise vectors, respectively,

with $\tilde{\mathbf{h}} \sim \mathcal{N}(\mathbf{0}, \mathbf{R}_{\tilde{\mathbf{h}}})$, and $\tilde{\mathbf{n}} \sim \mathcal{N}(\mathbf{0}, N_0\,\mathbf{I}_L)$. We denote the elements of $\tilde{\mathbf{h}}$ as (original) *branches*, and we assume them to be perfectly-known further in this section, unless stated otherwise.

The correlation matrix $\mathbf{R}_{\tilde{\mathbf{h}}} \stackrel{\triangle}{=} E\{\tilde{\mathbf{h}}\,\tilde{\mathbf{h}}^{\mathcal{H}}\}$ is Hermitian, i.e., $\mathbf{R}_{\tilde{\mathbf{h}}} = \mathbf{R}_{\tilde{\mathbf{h}}}^{\mathcal{H}}$, and therefore has real non-negative eigenvalues $\lambda_1 \geq \lambda_2 \geq \ldots \geq \lambda_L \geq 0$, and a complete set of orthonormal eigenvectors, $\mathbf{e}_i$, $i = 1 : L \stackrel{\triangle}{=} 1, \ldots, L$. Then, $\mathbf{R}_{\tilde{\mathbf{h}}} = \mathbf{E}_L \mathbf{\Lambda}_L \mathbf{E}_L^{\mathcal{H}}$, where $\Lambda_L \stackrel{\triangle}{=} \text{diag}\{\lambda_i\}_{i=1}^{L}$ is a diagonal matrix and $\mathbf{E}_L \stackrel{\triangle}{=} [\mathbf{e}_1\,\mathbf{e}_2\,\ldots\,\mathbf{e}_L]$ is a unitary matrix, i.e., $\mathbf{E}_L\,\mathbf{E}_L^{\mathcal{H}} = \mathbf{E}_L^{\mathcal{H}}\,\mathbf{E}_L = \mathbf{I}_L$. Throughout this work we assume that $\mathbf{\Lambda}_L$ and $\mathbf{E}_L$ are perfectly-known.

Maximal-ratio eigen-combining (MREC) of order N, $1 \leq N \leq L$ consists of two steps:

1) First, the $L \times N$ matrix $\mathbf{E}_N \stackrel{\triangle}{=} [\mathbf{e}_1\,\mathbf{e}_2\,\ldots\,\mathbf{e}_N]$ of full column rank, with $\mathbf{E}_N^{\mathcal{H}}\,\mathbf{E}_N = \mathbf{I}_N$ but $\mathbf{E}_N\,\mathbf{E}_N^{\mathcal{H}} \neq \mathbf{I}_L$, is used to apply the KLT to (1) and obtain the transformed signal vector

$$\mathbf{y} = \sqrt{E_b}\,b\,\mathbf{h} + \mathbf{n}, \tag{2}$$

where $\mathbf{y} \stackrel{\triangle}{=} \mathbf{E}_N^{\mathcal{H}}\tilde{\mathbf{y}}, \mathbf{h} \stackrel{\triangle}{=} \mathbf{E}_N^{\mathcal{H}}\tilde{\mathbf{h}}, \mathbf{n} \stackrel{\triangle}{=} \mathbf{E}_N^{\mathcal{H}}\tilde{\mathbf{n}}$. The elements $h_i \stackrel{\triangle}{=} \mathbf{e}_i^{\mathcal{H}}\,\tilde{\mathbf{h}}$, $i = 1 : N$, of $\mathbf{h}$ are further referred to as *eigen-branches* [3], and are also assumed perfectly-known unless stated otherwise. Vector $\mathbf{y}$ contains the projections of the original vector $\tilde{\mathbf{y}}$ on the N eigenvectors corresponding to the largest eigenvalues of $\mathbf{R}_{\tilde{\mathbf{h}}}$, i.e., $y_i \stackrel{\triangle}{=} \mathbf{e}_i^{\mathcal{H}}\,\tilde{\mathbf{y}} = \sqrt{E_b}\,b\,h_i + n_i$, where $h_i \stackrel{\triangle}{=} \mathbf{e}_i^{\mathcal{H}}\,\tilde{\mathbf{h}}$ and $n_i \stackrel{\triangle}{=} \mathbf{e}_i^{\mathcal{H}}\,\tilde{\mathbf{n}}$, $i = 1 : N$. Of all possible transforms the KLT is the optimum least-squares decorrelating transform [11] since it packs the largest amount of energy from the original signal vector $\tilde{\mathbf{h}}$ of dimension L into the the new vector $\mathbf{h}$ of dimension $N \leq L$, and the eigen-branches are mutually uncorrelated each with variance

$$\sigma_{h_i}^2 \stackrel{\triangle}{=} E\{|h_i|^2\} = \lambda_i, \tag{3}$$

i.e., $\mathbf{R}_{\mathbf{h}} = \Lambda_N = \text{diag}\{\lambda_i\}_{i=1}^{N}$, for any branch distribution [11]. For our initial assumptions about the branches and the noise, $\mathbf{h} \sim \mathcal{N}(\mathbf{0}, \Lambda_N)$ so that the eigen-branches are independent, and $\mathbf{n} \sim \mathcal{N}(\mathbf{0}, N_0\,\mathbf{I}_N)$ [12].

2) The elements of $\mathbf{y}$ are linearly combined so that to maximize the instantaneous output SNR, i.e., using the maximal-ratio combining (MRC) criterion [4]. The corresponding combiner for the signal in (2) is

$$\mathbf{w}_{MREC} = \mathbf{h}. \tag{4}$$

For $N = 1$, MREC reduces to maximum average SNR beamforming [5] (Max-ASNR BF) for the original received signal vector, where the combiner is proportional to the eigenvector of $\mathbf{R}_{\tilde{\mathbf{h}}}$ corresponding to its largest eigenvalue. Max-ASNR BF can provide antenna gain of up to $10\,log_{10}L$ dB [2] [13] when the original branches are highly correlated, but no diversity gain [13] in scenarios with lower branch correlation [7].

It can be shown that for the case of perfect channel knowledge, MREC of order $N = L$, denoted further as full MREC, is equivalent to MRC for the original received signal vector (MRCO), so that for correlated original branches performance measures for MRCO can be derived by analyzing the equivalent full MREC operating on independent eigen-branches [12].

In the above discussion, we assumed perfect knowledge of the branches and eigen-branches for MRCO and MREC, respectively, which is unrealistic since these short-term channel parameters have to be estimated from the received signals. In this work we will consider that $\forall\, i = 1 : N$ the estimate $g_i = \hat{h_i}$ of the eigen-branch h_i is calculated from temporal samples of y_i, so that g_i and g_j are independent for $i \neq j$. Assume also that g_i is zero-mean, that g_i and h_i are jointly-Gaussian, $\forall i = 1 : N$, and define their correlation coefficient as [14]

$$\mu_i \stackrel{\triangle}{=} \frac{E\{h_i\, g_i^*\}}{\sqrt{E\{|h_i|^2\}\, E\{|g_i|^2\}}} = \frac{\sigma^2_{h_i,g_i}}{\sqrt{\sigma^2_{h_i}\, \sigma^2_{g_i}}} = \frac{\sigma^2_{h_i,g_i}}{\sqrt{\lambda_i\, \sigma^2_{g_i}}} \tag{5}$$

and assume it to be real-valued [15, Appendix C].

Generally, branch/eigen-branch estimates are used as actual combiner weights — e.g., for MRCO in [15, Appendix C] [16] [17], and for MREC in [9] [10] — which is suboptimal in the maximal-ratio sense. We will analyze *approximate* MREC (AMREC) in Section III. For estimated independent branches, the optimal combining method in the maximal-ratio sense is analyzed in [14] for MRCO. Applying results from [14] for *exact* MREC (EMREC) leads us to propose a novel criterion which may enable a smart antenna array to adaptively select the most appropriate number of dominant eigen-branches in MREC for any channel features, as is described in Section V.

The remaining of this section consists of a description of channel estimation using pilot-symbol-aided modulation (PSAM) and interpolation. The results shown next will be used to specialize the general analysis presented in further sections.

In pilot-symbol-aided modulation (PSAM) the transmitter periodically inserts pilot symbols into the data symbol stream. The receiver then estimates the fading gain by interpolating the pilot samples acquired across frames [18]. The notation (t, m) is used to denote temporal

TABLE I

CORRELATIONS REQUIRED FOR μ_i IN (5)

$\sigma^2_{h_i}$	λ_i
$\sigma^2_{h_i,g_i}$	$\boldsymbol{\phi}_i(m)^{\mathcal{H}}\,\mathbf{v}_i(m)$
$\sigma^2_{g_i}$	$\mathbf{v}_i(m)^{\mathcal{H}}\,\boldsymbol{\Phi}_i\,\mathbf{v}_i(m)$

TABLE II

ELEMENTS OF $\boldsymbol{\Phi}_i$ AND $\boldsymbol{\phi}_i(m)$

$[\boldsymbol{\Phi}_i]_{t_1,t_2}$	$\lambda_i\,J_0\left(2\pi f_n\,\lvert t_1-t_2\rvert\,M\right)+\frac{N_0}{E_b\lvert b_p\rvert^2}\delta_{t_1,t_2}$
$[\boldsymbol{\phi}_i(m)]_t$	$\lambda_i\,J_0\left(2\pi f_n\,\lvert tM-m\rvert\right)$

indexing, where $t=-T_1:T_2$ is the frame index, t = 0 corresponds to the frame in which estimation takes place, $T=T_1+T_2+1$ frames are used for interpolation, $m=0:M-1$ is the symbol index within the frame, where $m=0$ corresponds the pilot symbol and M is the frame length. For MREC, the estimate of the ith eigen-branch at the mth data symbol position in the current frame can be written based on [18] as

$$g_i\left(0,m\right)=\mathbf{v}_i(m)^{\mathcal{H}}\,\mathbf{r}_i, \tag{6}$$

where $\mathbf{v}_i(m)$ contains the interpolation coefficients and is denoted as the PSAM interpolation filter, and $\mathbf{r}_i$ is a vector formed with the pilot signal samples:

$$\mathbf{r}_i\stackrel{\triangle}{=}\frac{1}{\sqrt{E_b}\,b_p}\left[y_i\left(-T_1,0\right)\,\ldots\,y_i\left(T_2,0\right)\right]^{\mathcal{T}}, \tag{7}$$

with b_p the pilot symbol, and $y_i\left(t,0\right)=\mathbf{e}_i^{\mathcal{H}}\,\tilde{\mathbf{y}}\left(t,0\right)$. The correlations required to compute μ_i from (5) are determined based on (6) and (7) and are shown in Table I, where $\boldsymbol{\Phi}_i\stackrel{\triangle}{=}E\{\mathbf{r}_i\,\mathbf{r}_i^{\mathcal{H}}\}$ and $\boldsymbol{\phi}_i(m)\stackrel{\triangle}{=}E\{\mathbf{r}_i\,h_i^*\left(0,m\right)\}$. For Jakes' model of temporal correlation [19], we express the elements of $\boldsymbol{\Phi}_i$ and $\boldsymbol{\phi}_i(m)$ in Table II, where $J_0(\cdot)$ is the zeroth-order Bessel function of the first kind and f_n is the normalized maximum Doppler rate.

The interpolation filters can be classified as:

1) **data-independent**, e.g., the SINC filter with brick-wall-type frequency response, which is optimum in the absence of noise; we taper its time-response with a raised-cosine window [20], and denote the corresponding estimation approach as SINC PSAM.

TABLE III

INTERPOLATION FILTERS

SINC	$[\mathbf{v}\,(m)]_t = \text{sinc}(\frac{m}{M} - t)\frac{\cos\left[\pi\beta(\frac{m}{M}-t)\right]}{1-\left[2\beta(\frac{m}{M}-t)\right]^2}$
MMSE	$\mathbf{v}_i\,(m) = \mathbf{\Phi}_i^{-1}\,\boldsymbol{\phi}_i(m)$

2) **data-dependent**, e.g., the Wiener filter, which is minimum mean-squared error (MMSE) optimum in the presence of noise, but requires the second-order statistics of the received signals [18]; this filter is referred to as the MMSE filter, and the corresponding channel estimation approach as MMSE PSAM.

Table III specifies the SINC [20] and MMSE [18] interpolation filters, where $\text{sinc}(x) = \frac{\sin \pi\, x}{\pi\, x}$, and β is the raised-cosine rolloff factor ($\beta = 0.2$ for the numerical results shown later).

III. APPROXIMATE MREC (AMREC) - PERFORMANCE ANALYSIS

In this section, we analyze the approximate MREC method for BPSK and Rayleigh fading. In this case, the combiner weights are [9] [10]:

$$[\mathbf{w}_A]_i = g_i, \quad i = 1 : N. \tag{8}$$

It was shown in [17] that the distribution of the instantaneous output SNR is insufficient for finding the AEP for the approximate maximal-ratio combining approach for BPSK modulation. Instead, the decision variable for symbol detection has to be used [16] [9] [21], so that our AMREC analysis starts with

$$q \stackrel{\triangle}{=} \Re\left\{\sum_{i=1}^{N} g_i^*\, y_i\right\} = \sum_{i=1}^{N} \Re\left\{g_i^*\, y_i\right\} = \sum_{i=1}^{N} q_i, \tag{9}$$

where the random variables $q_i \stackrel{\triangle}{=} \Re\{g_i^*\, y_i\}$, $i = 1 : N$, are mutually independent.

The AMREC AEP-expressions shown next have been derived using the following procedure:

1) for $b = 1$, the moment generating function (MGF) of q_i, $M_{q_i}(s) \stackrel{\triangle}{=} E\{e^{-s\,q_i}\}$, is computed (alternatively, [9] [16] [21] used the characteristic function).
2) since q_i are independent, $i = 1 : N$, the MGF of q is determined as $M_q(s) \stackrel{\triangle}{=} E_q\{e^{-s\,q}\} = \prod_{i=1}^{N} M_{q_i}(s)$, based on (9).

3) a partial fraction expansion of $M_q(s)$ may then be necessary before its inverse Laplace transform is taken, thus leading to the PDF of q, $p_q(q)$.
4) the AEP is calculated as $P_e = \int_{-\infty}^{0} p_q(q)\,\mathrm{d}q$.

In general, some eigen-branches may be identically distributed since their corresponding eigenvalues may coincide. For the rest of this section, let the index denote distinctly-distributed eigen-branches so that $\lambda_1 > \lambda_2 > \ldots > \lambda_K$ are the $K \leq N$ distinct eigenvalues, with algebraic multiplicities $r_1, r_2, \ldots, r_K$, respectively, where $\sum_{k=1}^{K} r_k = N$. Then, the steps 1) and 2) above produce:

$$M_q(s) = \prod_{k=1}^{K} \frac{1}{\left[-a_k^2 (s - s_{k,1})(s + s_{k,2})\right]^{r_k}} \tag{10}$$

where $a_k^2 = \frac{1}{4} N_0 \, \sigma_{g_k}^2 \left[1 + \frac{E_b}{N_0} \lambda_k \left(1 - \mu_k^2\right)\right]$, and

$$s_{k,\{1,2\}} = \frac{2\nu_k}{\sqrt{E_b \, \lambda_k \, \sigma_{g_k}^2}} \cdot \frac{1}{1 \mp \mu_k \, \nu_k} \tag{11}$$

are both real and positive, with $\nu_k = \sqrt{\frac{\Gamma_k}{\Gamma_k + 1}}$ with $\Gamma_k = \frac{E_b}{N_0} \lambda_k$.

The MGF in (10) is more conveniently rewritten as:

$$M_q(s) = \frac{1}{B} \prod_{p=1}^{2K} \frac{1}{(s + \sigma_p)^{\rho_p}} \tag{12}$$

where $B = \prod_{k=1}^{K} (-a_k^2)^{r_k}$, $\sigma_p = -s_{p,1}$, $\rho_p = r_p$ for $p = 1 : K$, and $\sigma_p = s_{p-K,2}$, $\rho_p = r_{p-K}$ for $p = K+1 : 2K$. Based on [22, ¶2.102, pp. 56-57], the partial fraction expansion for the MGF in (12) is

$$M_q(s) = \frac{1}{B} \sum_{p=1}^{2K} \sum_{l=1}^{\rho_p} c_{p,l} \frac{1}{(s + \sigma_p)^l}, \tag{13}$$

and its coefficients may be calculated based on [22] [23] to be

$$\begin{aligned} c_{p,l} &\triangleq \frac{B}{(\rho_p - l)!} \left\{ D_s^{(\rho_p - l)} \left[M_q(s) \cdot (s + \sigma_p)^{\rho_p} \right] \right\} |_{s=-\sigma_p}, \\ &= (-1)^{\rho_p - l} \cdot \sum_{\substack{0 \leq i_1, \ldots, i_{p-1}, i_{p+1}, \ldots, i_{2K} \leq \rho_p - l \\ i_1 + \ldots + i_{p-1} + i_{p+1} + \ldots + i_{2K} = \rho_p - l}} \prod_{\substack{j=1 \\ j \neq p}}^{2K} \binom{\rho_j - 1 + i_j}{i_j} \frac{1}{\left(\sigma_j - \sigma_p\right)^{(\rho_j + i_j)}}. \end{aligned} \tag{14}$$

The PDF of q can be obtained as the inverse Laplace transform of (13):

$$p_q(q) = \frac{1}{B} \sum_{k=1}^{K} \sum_{l=1}^{r_k} \left[-\frac{c_{k,l}}{(l-1)!} q^{l-1} e^{s_{k,1} \, q} \, u(-q) + \frac{c_{k+K,l}}{(l-1)!} q^{l-1} e^{-s_{k,2} \, q} \, u(q) \right], \tag{15}$$

where $u(q) = 0$ for $q < 0$, and $u(q) = 1$ for $q \geq 0$. Then the average error probability (AEP) for AMREC of order N can be shown to have the following expression:

$$P_e = \frac{1}{B} \sum_{k=1}^{K} \sum_{l=1}^{r_k} c_{k,l} \left(-\frac{\sqrt{E_b \, \sigma_{h_k}^2 \, \sigma_{g_k}^2}}{\nu_k} \right)^l \left[\frac{1}{2} \left(1 - \mu_k \, \nu_k \right) \right]^l . \tag{16}$$

This novel formula is applicable for any correlations between the original branches and for any channel estimation method which satisfies the assumptions made earlier for the distribution of the eigen-branches and their corresponding estimates (i.e., zero mean, jointly-Gaussian random variables). AMREC AEP plots obtained by specializing the above formula to SINC and MMSE PSAM channel estimation using the results from Section II will be discussed in Section VI.

For equal-variance eigen-branches we can drop the index k since $k = K = 1$ ($r_1 = N$). Manipulating (16) and (14), we obtain:

$$P_e = \left[\frac{1}{2} \left(1 - \mu \, \nu \right) \right]^N \sum_{n=0}^{N-1} \binom{N-1+n}{n} \left[\frac{1}{2} \left(1 + \mu \, \nu \right) \right]^n . \tag{17}$$

This can be shown to coincide with [16, Eqn. 59], if the latter is written for the independent eigen-branches. For perfectly-known channels we have $\mu = 1$ and (17) reduces to the well-known result [15, Eqn. (14.4-15)], if the latter is written for the independent eigen-branches.

When all eigen-branches have distinct variances ($K = N$ and $r_k = 1$, $\forall k = 1 : N$) then (16) and (14) yield:

$$P_e = \frac{1}{2} \sum_{k=1}^{N} S_k \cdot \left(1 - \mu_k \, \nu_k \right) , \tag{18}$$

where

$$S_k = \prod_{\substack{j=1 \\ j \neq k}}^{N} \frac{1}{a_j^2 (s_{j,1} - s_{k,1})(s_{j,2} + s_{k,1})} . \tag{19}$$

Previously, an AMREC-AEP expression was derived for unequal eigen-branch variances (eigenvalues) [9], but it applies only to maximum likelihood (ML) channel estimation. Clearly, the ML estimate — see [9, eqns. (3),(4)] or [10, eqns. (6),(7),(9)] — can be written similarly to (6) where the elements of $\mathbf{v}_i$ are all equal to 1, and $\mathbf{r}_i$ contains successive samples of y_i. Therefore, our formula (16) can reproduce the expression in [9, Eqn. (16)] since it is more general.

Note that for perfect channel knowledge (18) and (19) reduce to the well-known [15, Eqn. (14.5-28)] and [15, Eqn. (14.5-27)], respectively, if the latter are written for the independent eigen-branches.

The AEP-expressions derived above hold for Max-ASNR BF. They obviously also hold for AMRCO if the original branches are uncorrelated since then the KLT does not have any effect, which makes AMREC and AMRCO identical. We show next that AMREC may be equivalent to AMRCO even for correlated branches.

Proposition: for estimated branches and eigen-branches, AMRCO is equivalent to full AMREC if and only if [1]:

$$\widehat{\mathbf{E}_L^{\mathcal{H}}\tilde{\mathbf{h}}} = \mathbf{E}_L^{\mathcal{H}}\widehat{\tilde{\mathbf{h}}}. \tag{20}$$

The proof follows easily by imposing the equality between the combiners' outputs for AMRCO and AMREC.

Clearly, if the original branches are uncorrelated then $\mathbf{E}_L = \mathbf{I}_L$ in (20), and the above AEP-expressions describe AMRCO for independent branches with unequal or equal variances, for any estimation method. For data-independent interpolation filters (such as ML or SINC) straightforward calculations can show that (20) is satisfied, which makes full AMREC equivalent to AMRCO and the above AEP-expressions with $N = L$ apply for AMRCO. For (data-dependent) MMSE interpolation we found through slightly more complicated calculations that (20) is not satisfied, so that full AMREC is not equivalent to AMRCO.

Since full AMREC AEP does not always provide the AMRCO AEP, which would be required for a comparison of various combining methods, we derived the latter using instead the procedure from [21, Section III] to determine the MGF of the symbol detection variable, and then the procedure described above by equations (12)–(16). The AMRCO AEP expression (not shown, to save space) was specialized for both SINC and MMSE PSAM and will be used in Section VI.

IV. EXACT MREC (EMREC) - PERFORMANCE ANALYSIS

Based on [14] where exact MRCO (EMRCO) of uncorrelated and imperfectly-estimated branches was analyzed, we now analyze exact MREC. First, one can show that the instantaneous SNR conditioned on the estimate g_i of the ith eigen-branch is [14]

$$\gamma_i = \frac{\frac{E_b}{N_0}\lambda_i|\mu_i|^2}{\frac{E_b}{N_0}\lambda_i\left(1-|\mu_i|^2\right)+1} \cdot \frac{|g_i|^2}{\sigma_{g_i}^2}. \tag{21}$$

[1] $\hat{\cdot}$ denotes an estimator

Denote as γ the instantaneous SNR in $\mathbf{w}^{\mathcal{H}}\,\mathbf{y}$ for some combiner $\mathbf{w}$. Given the eigen-branch estimates, the combiner weights [14]

$$[\mathbf{w}_E]_i = \frac{\frac{E_b}{N_0}\,\mu_i\,\sqrt{\lambda_i/\sigma_{g_i}^2}}{\frac{E_b}{N_0}\,\lambda_i\,(1-|\mu_i|^2)+1}\,g_i, \quad i=1:N, \tag{22}$$

will maximize γ, i.e. [4] [14]

$$\gamma = \sum_{i=1}^{N}\gamma_i, \tag{23}$$

which can now be used for performance analysis [14]. Note the difference between the weights for EMREC and AMREC given by (22) and (8), respectively.

The average error probability (AEP) for EMREC of order N is then [15]

$$P_{e,N} = E\{P_e(\gamma)\} = \int_0^\infty P_e(\gamma)\,p_t(\gamma)\,\mathrm{d}\gamma, \tag{24}$$

where $p_t(\gamma)$ is the probability density function (PDF) of the total instantaneous SNR γ.

For BPSK, it can be shown that (24) becomes [24]

$$P_{e,N} = \frac{1}{\pi}\int_0^{\pi/2} M_\gamma\left(\frac{1}{\sin^2\phi}\right)\mathrm{d}\phi, \tag{25}$$

with $M_\gamma(s) \stackrel{\triangle}{=} E\{e^{-s\gamma}\}$, the MGF of γ.

Since g_i is zero-mean and Gaussian, γ_i is exponentially distributed [4], i.e., with PDF

$$p(\gamma_i) = \frac{1}{\Gamma_i'}\,e^{-\gamma_i/\Gamma_i'}, \tag{26}$$

where the average eigen-branch SNR conditioned on g_i is, based on (21):

$$\Gamma_i' \stackrel{\triangle}{=} E\{\gamma_i\} = \frac{\frac{E_b}{N_0}\lambda_i|\mu_i|^2}{\frac{E_b}{N_0}\lambda_i\,(1-|\mu_i|^2)+1} \tag{27}$$

Then [24]

$$M_{\gamma_i}(s) \stackrel{\triangle}{=} E_{\gamma_i}\{e^{-s\,\gamma_i}\} = \frac{1}{1+s\,\Gamma_i'} \tag{28}$$

and, since γ_i, $i=1:N$ are independent, the MGF of γ is

$$M_\gamma(s) = \prod_{i=1}^{N}\left(\frac{1}{1+s\,\Gamma_i'}\right). \tag{29}$$

Note that this reduces to [25, Eqn. (10-59)] for the case of perfect channel knowledge.

From (29) and (25), the AEP-expression for order-N EMREC is

$$P_{e,N} = \frac{1}{\pi}\int_0^{\pi/2}\prod_{i=1}^{N}\left(\frac{\sin^2\phi}{\sin^2\phi+\Gamma_i'}\right)\mathrm{d}\phi. \tag{30}$$

In Section VI numerical integration will allow evaluation of symbol detection performance for EMREC (thus also Max-ASNR BF, when $N = 1$). This formula can be used to select the MREC order, as will be shown in Section V.

While full AMREC and AMRCO may be equivalent for certain channel estimation methods (as discussed in the last part of Section III), a relationship between full EMREC and EMRCO was not found. Although the EMRCO AEP can be found using the same procedure as for AMRCO as described in Section III, this is unnecessary since in Section VI we are to specialize all these formulas for antenna arrays. In such a case, for most channel models [1] [7] [8] [26] all branches $\tilde{h}_i, i = 1 : L$ have the same variance, which makes the (real-valued) factors multiplying the branch estimates for EMRCO [14] coincide, so that EMRCO is equivalent to AMRCO.

Full MREC and MRCO are always equivalent for perfectly-known channels [12]. Therefore, if $\mu_i = 1$ then (30) with $\Gamma_i' = \frac{E_b}{N_0}\lambda_i$ represents the MRCO AEP-expression for BPSK modulation and perfectly-known Rayleigh fading branches which may be correlated and with distinct variances. It can be used to show that uncorrelated and identically distributed branches minimize AEP, while coherent branches maximize AEP for MRCO. The opposite can be shown for Max-ASNR BF (for perfect channel knowledge) using (30) for $N = 1$.

V. ORDER SELECTION FOR MREC

In this section we first describe two MMSE-based criteria employed previously for reduced-rank processing [27] and order selection for AMREC [10], and we outline their disadvantages. Then, based on the EMREC AEP-expression, we propose a new order-selection criterion which trades-off detection performance versus short-term processing complexity.

The MREC order may be determined based on the following MMSE criterion proposed by Scharf in [28]:

$$\min_{N=1:L} E\left\{\|\tilde{\mathbf{y}} - \mathbf{E}_N\,\mathbf{E}_N^{\mathcal{H}}\,\tilde{\mathbf{y}}\|^2\right\}. \tag{31}$$

This criterion can be further written as [28]

$$\min_{N=1:L}\left[\sum_{i=N+1}^{L}\lambda_i + N\cdot N_0\right] \tag{32}$$

and is known as the *bias-variance tradeoff* criterion [27] because it trades-off the error due to removal of intended-signal components with the weakest contribution vs. the reduction in noise variance due to the removal of the corresponding noise components.

TABLE IV

AMREC ORDER-SELECTION CRITERION IN (33) FOR SINC AND MMSE PSAM

SINC	$\min_{N=1:L}\left\{\sum_{i=1}^{L}\lambda_i-\sum_{i=1}^{N}\mathbf{v}(m)^{\mathcal{H}}\boldsymbol{\phi}_i(m)-\sum_{i=1}^{N}\boldsymbol{\phi}_i(m)^{\mathcal{H}}\mathbf{v}(m)+\sum_{i=1}^{N}\mathbf{v}(m)^{\mathcal{H}}\boldsymbol{\Phi}_i\mathbf{v}(m)\right\}$
MMSE	$\min_{N=1:L}\left\{\sum_{i=1}^{L}\lambda_i-\sum_{i=1}^{N}\boldsymbol{\phi}_i(m)^{\mathcal{H}}\boldsymbol{\Phi}_i^{-1}\boldsymbol{\phi}_i(m)\right\}=L$

Scharf's bias-variance tradeoff criterion only provides a lower-rank approximation of the initial received signal vector and does not account for the actual estimation method or the number of pilot symbols employed. To address this issue, Dietrich et al. [10] proposed finding the order for AMREC using the following MMSE criterion:

$$\min_{N=1:L} E\left\{\|\tilde{\mathbf{h}}-\mathbf{E}_N\,\hat{\mathbf{h}}\|^2\right\}. \tag{33}$$

Although this criterion was successfully applied in [10] for ML-estimated eigen-branches, assuming a constant channel over the training period, we found it unapplicable in other cases as described below. For PSAM-based eigen-branch estimation using (6) simple calculations show that the criterion in (33) becomes

$$\min_{N=1:L}\left\{\sum_{i=1}^{L}\lambda_i-\sum_{i=1}^{N}\mathbf{v}_i(m)^{\mathcal{H}}\boldsymbol{\phi}_i(m)-\sum_{i=1}^{N}\boldsymbol{\phi}_i(m)^{\mathcal{H}}\mathbf{v}_i(m)+\sum_{i=1}^{N}\mathbf{v}_i(m)^{\mathcal{H}}\boldsymbol{\Phi}_i\mathbf{v}_i(m)\right\}, \tag{34}$$

which for the SINC and MMSE interpolation filters in Table III yields the corresponding criteria given in Table IV. In Section VI we will see that for correlated branches and SINC PSAM the corresponding criterion in Table IV yields $N<L$ for significant branch correlation. However, for MMSE PSAM, Tables III and I show that $\boldsymbol{\phi}_i(m)^{\mathcal{H}}\boldsymbol{\Phi}_i^{-1}\boldsymbol{\phi}_i(m)=\mathbf{v}_i(m)^{\mathcal{H}}\boldsymbol{\Phi}_i\,\mathbf{v}_i(m)=\sigma_{g_i}^2\stackrel{\triangle}{=}E\{|g_i|^2\}\geq 0$ and therefore the corresponding criterion in Table IV always yields $N=L$ regardless of the branch correlation and noise variance. Thus, for MMSE PSAM-based eigen-branch estimation, efficient selection of the MREC order is not possible using Dietrich's criterion.

Dietrich's criterion was also found to underestimate the AMREC order compared to the order which minimizes the BER (obtained by simulations) for ML estimation [10]. While an underestimated order reduces the complexity of the receiver, it may also lead to poor detection performance, as we will see for SINC PSAM in Section VI.

The above disadvantages can be avoided by using the EMREC AEP-expression (30) as shown next. Assume that Γ_i', $i=1:L$, are all known from (27) and ordered as follows:

$\Gamma'_1 \geq \Gamma'_2 \geq \ldots \geq \Gamma'_L \geq 0$. It is clear from (27) that the AEP-performance of order-N EMREC will never degrade by introducing the $(N+1)$st strongest eigen-branch, i.e., $P_{e,N+1} \leq P_{e,N}$, $\forall\, N \leq L-1$ (full EMREC always has the lowest AEP). However, the performance gain associated with an extra eigen-branch in EMREC may be too small to justify the increased complexity. Therefore, we propose the following criterion: $(N+1)$ dominant eigen-branches should be used instead of N only if

$$P_{e,N+1} \leq \upsilon\, P_{e,N}, \tag{35}$$

i.e., if the presence of an additional eigen-branch decreases the AEP by a factor $\upsilon \in (0,1)$. If we define the cutoff eigen-branch average SNR as $\Gamma'_c \stackrel{\triangle}{=} \frac{1}{\upsilon} - 1$ then, using (35) and (30), it can easily be shown that

$$\Gamma'_{N+1} \geq \Gamma'_c \tag{36}$$

is a *sufficient condition* for the AEP-inequality in (35) to hold. In an actual system the factor $\upsilon \in (0,1)$ should be used as a design parameter to trade-off detection performance vs. complexity. Inappropriate selection of υ can lead to the following situations: if υ is chosen too large then weak eigen-branches are considered for MREC, which insignificantly improve the detection performance at the expense complexity; if υ is chosen too small then too much weight is placed on complexity reduction over detection performance.

The following limiting cases are possible for the criterion in (35):

- if $\Gamma'_1 \geq \Gamma'_2 \geq \ldots \geq \Gamma'_L \geq \Gamma'_c$ then full EMREC is the best choice.
- if $\Gamma'_1 \geq \Gamma'_c > \Gamma'_2 \geq \ldots \geq \Gamma'_L$ then Max-ASNR BF is the best choice.

The numerical results from Section VI will show good performance when applying our criterion for EMREC and even for AMREC. Note that the new criterion in (35) is intended to select between Max-ASNR BF and higher-order MREC when the branch inter-correlation is significant. This criterion is not for choosing between MREC and MRCO in general, although it may work when full MREC and MRCO are equivalent (as for AMREC with data-independent interpolation in PSAM — ML or SINC), as seen in Section VI.

Our criterion is reminiscent of hybrid selection combining/MRC [14] [24] (HSC/MRC). While HSC/MRC selects the strongest (in short-term, instantaneous) branches, MREC with our criterion selects the strongest (in long-term, averaging over fading) eigen-branches. Our criterion is also reminiscent of the way dominant fingers are selected for further processing in a RAKE receiver [26, Section 3.3.3].

Finally, note that the discussed methods for MREC tuning can all be applied adaptively in smart antenna array systems, but the newly-proposed criterion is general, accounts for the estimation method and its parameters, and trades-off performance vs. complexity through a parameter chosen by the system designer, unlike Scharf's and Dietrich's criteria.

VI. NUMERICAL RESULTS

Herein, we make use of the MREC AEP-expressions (16) and (30), and AEP-expressions for MRCO, when the vector $\tilde{\mathbf{y}}$ in (1) consists of signals received at a uniform linear antenna array (ULA) with $L = 5$ elements and inter-element distance equal to half of the carrier wavelength. Unless otherwise stated, a single scattering region is assumed with central angle of arrival (AOA) $\theta_c = 0^\circ$ (broadside). The AOA is considered to have Laplacian distribution, which fits actual measurements [1]. The standard deviation, or angle spread, is denoted as σ_{AS}.

A. The effect of angle spread on combining performance

For the channel model described in [1], the eigenvalues λ_i, $i = 1 : L$ of the channel correlation matrix and the fading correlation between any two adjacent elements, $\rho_{1,2}$, are plotted in Fig. 1 vs. angle spread. Notice that for small σ_{AS} the received signals are highly correlated so that the signal energy, i.e., $\text{tr}(\mathbf{R_h}) = \sum_{i=1}^{L} \lambda_i$, is concentrated in the first few eigenvalues, and then the available diversity gain is small [13]. As the angle spread increases, the inter-branch correlation decreases, the channel becomes spatially more selective and higher diversity gain is available. Notice also that several eigenvalues can be almost equal at certain angle spread values.

The results shown next are for symbol-SNR $E_b/N_0 = 5$ dB and normalized maximum Doppler rate $f_n = 0.05$, for which $M = 7$ and $T = 11$ ($T_1 = T_2 = 5$) are appropriate parameter choices for PSAM and interpolation [18]. For $N = 1$, EMREC reduces to the low-complexity Max-ASNR BF approach. While Max-ASNR BF has the lowest AEP for very small σ_{AS}, the detection performance may degrade dramatically as σ_{AS} becomes larger, as shown in Fig. 2 for SINC PSAM. To avoid this problem one could take advantage of the available diversity gain by using EMREC with two or more eigen-branches [7], at an increased complexity.

Given the EMREC order, $1 < N < L$, the AEP decreases with increasing σ_{AS} as long as the signal subspace has smaller dimension than N. The AEP-curve minimum occurs when

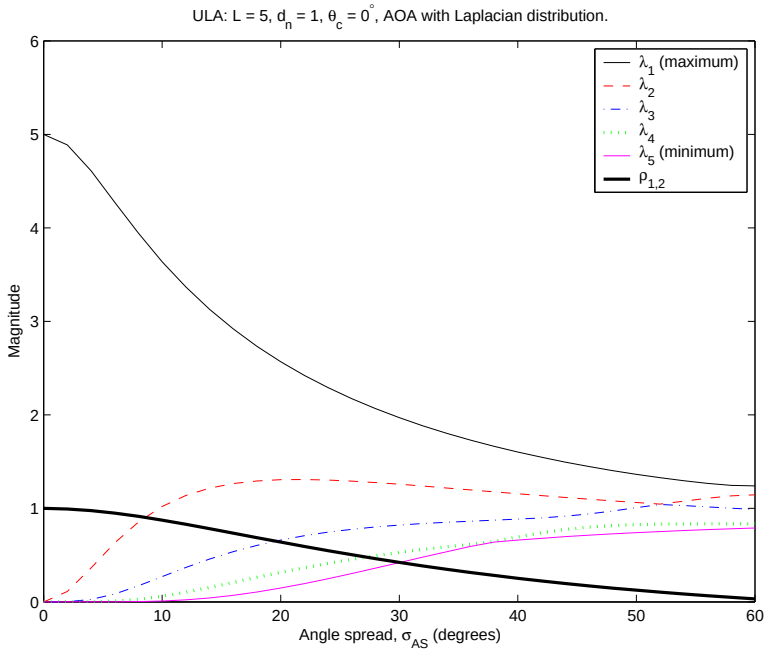

Fig. 1. The eigenvalues λ_i, $i = 1 : L$, of the channel vector correlation matrix $\mathbf{R}_{\tilde{\mathbf{h}}}$, and the fading correlation coefficient $\rho_{1,2}$ at any two adjacent antenna elements vs. the angle spread σ_{AS}, for the channel model in [1] with Laplacian AOA distribution.

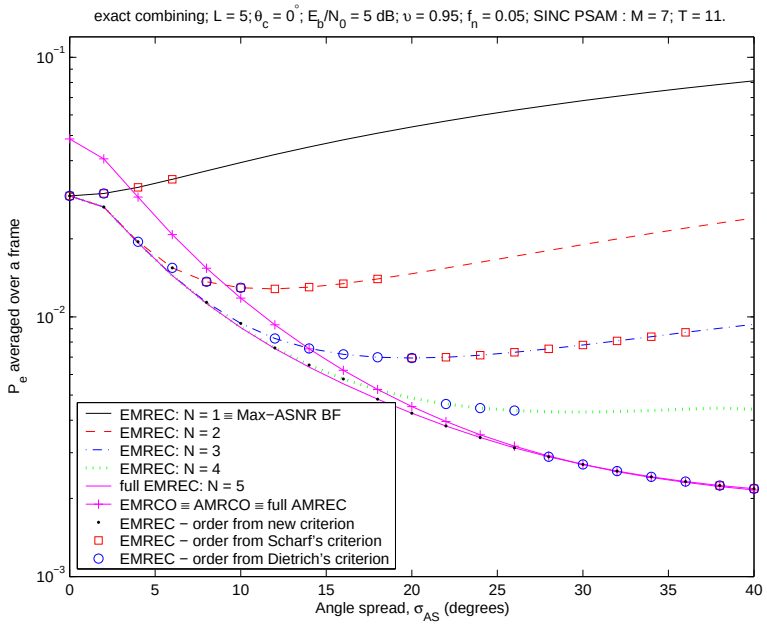

Fig. 2. AEP vs. the angle spread for exact combining and SINC PSAM channel estimation; (30) is used for EMREC.

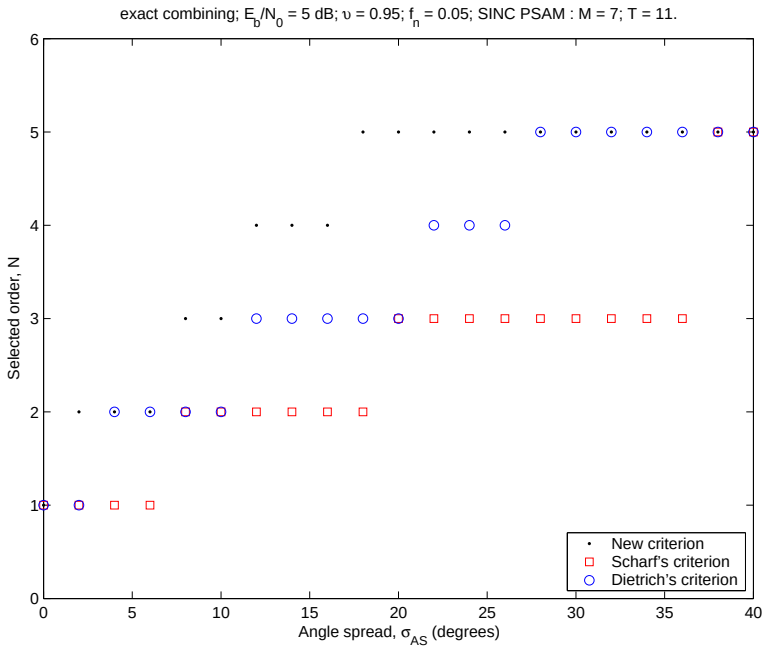

Fig. 3. Selected EMREC order vs. the angle spread, for the three criteria described in Section V, for SINC PSAM channel estimation.

the potential diversity gain for the chosen N is realized. The AEP starts degrading when N is smaller than the signal subspace dimension, and MREC inappropriately discards intended signal energy.

Notice also that EMREC of order $N < L$ yields minimum AEP up to a certain angle spread value which increases with greater N. This is a direct consequence of the eigenvalue dependence on angle spread (see Fig. 1) and its effect on the average eigen-branch SNRs from (27) which appear in the EMREC AEP-expression (30).

Fig. 2 also shows that, for any given $N < L$, EMREC has lower AEP than that of EMRCO as long as the angle spread is small enough, and full EMREC performs at least as well as EMRCO for any angle spread. Their performances tend to coincide for large σ_{AS} because the branches become nearly uncorrelated and the KLT has a minimal effect, rendering EMREC almost identical to EMRCO.

Fig. 2 shows the AEP obtained with EMREC using the criteria described in Section V. Notice the nearly-minimum AEP obtained using the new criterion (for $\upsilon = 0.95$) compared to the other two criteria. Fig. 3 highlights the results from Fig. 2 to show that, while EMREC with various orders may have similar AEP, the new criterion selects the least complex

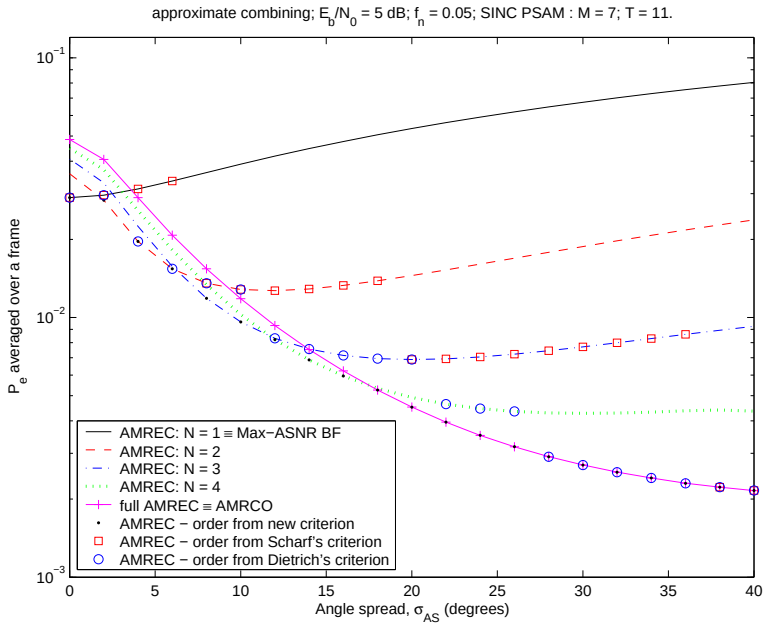

Fig. 4. AEP vs. the angle spread for approximate combining and SINC PSAM channel estimation; (16) is used for AMREC.

combiner. For example, for $\sigma_{AS} = 10°$, EMREC with $3 \leq N \leq L = 5$ has almost identical AEPs, but $N = 3$, i.e., the minimum required order, is selected. Figs. 2 and 3 show that Scharf's and Dietrich's criteria from (32) and (33), respectively, tend to underestimate the EMREC-order.

Similar results can be obtained for Max-ASNR BF/EMREC/EMRCO for MMSE PSAM channel estimation. One difference is that the corresponding curves are shifted slightly downwards. Another one is that the Dietrich's criterion in (33) always selects full EMREC, thus maximizing the complexity regardless of the angle spread, i.e., the actual branch correlation.

Note from Fig. 2 that, given the angle spread, overestimating the EMREC order N increases the complexity but cannot degrade the detection performance. Consider Fig. 4, describing the performance of approximate combining (AMREC, AMRCO) for SINC PSAM. The selection of AMREC order is critical because overestimating N can now increase complexity as well as degrade AEP performance. This behavior is determined by very low variance (eigenvalue) for several eigen-branches for small-to-moderate σ_{AS} (see Fig. 1), which causes the corresponding eigen-branch estimates, g_i, to be mainly due to the corresponding noise, n_i. Unless eliminated by an appropriate criterion, the noise-only estimate enters AMREC as in (8). In EMREC the

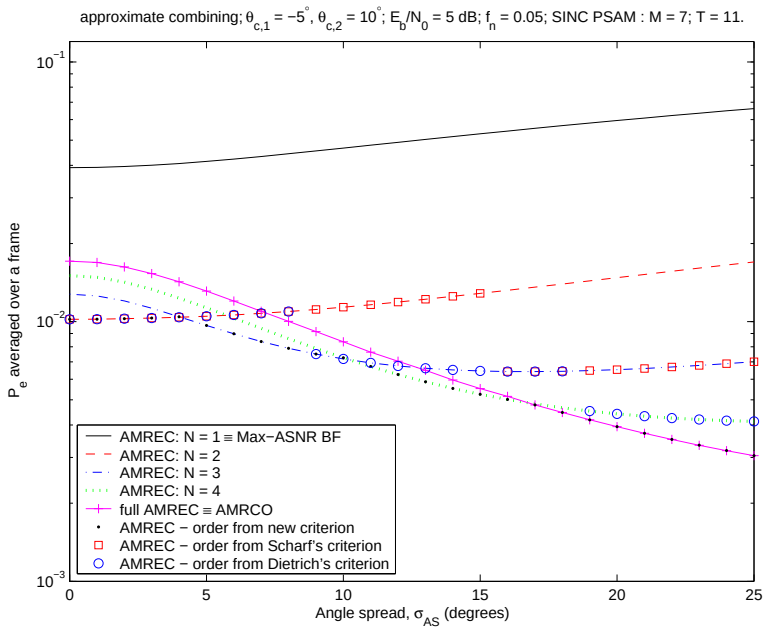

Fig. 5. AEP vs. the angle spread for approximate combining and SINC PSAM channel estimation, when 2 clusters of scatterers are present, one at $\theta_{c,1} = -5°$, the other at $\theta_{c,2} = 10°$; (16) is used for AMREC.

factors that multiply the eigen-branch estimates in (22) eliminate the contribution of noise-only eigen-branches in the combiner output, so that AEP-performance always improves by increasing the order of EMREC. Finally, Fig. 4 also shows that, although designed for exact combining, the criterion can still provide good performance for AMREC.

In other results not shown, we also observed that, for MMSE PSAM, the AEP-performance does not degrade with increasing AMREC-order since, for almost-zero eigenvalues, the interpolation filter coefficients from Tables III and II are almost zero, so that g_i approaches zero.

Finally, we consider the situation when 2 clusters of scatterers are present, one at $\theta_{c,1} = -5°$ and the other at $\theta_{c,2} = 10°$, each with the same σ_{AS}. Fig. 5 describes approximate combining for SINC PSAM, showing that a beamforming antenna is not adequate. However, our criterion can still select the least complex AMREC which yields nearly-minimum AEP, even outperforming AMRCO (equivalent to full AMREC for SINC PSAM) at small-to-moderate σ_{AS}.

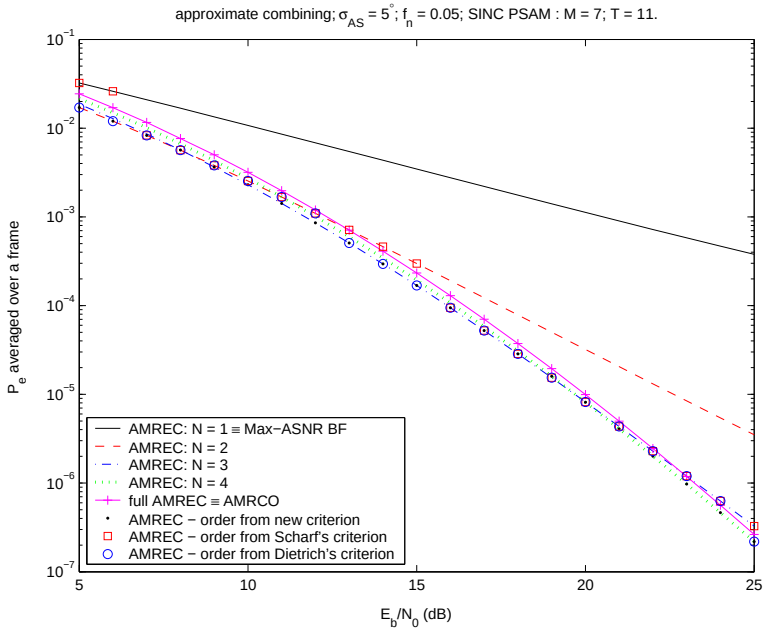

Fig. 6. AEP vs. the symbol SNR E_b/N_0, at $\sigma_{AS} = 5^\circ$, for approximate combining and SINC PSAM channel estimation; (16) is used for AMREC.

B. The effect of symbol-SNR on combining performance

Fig. 6 depicts the AEP for AMREC and AMRCO with SINC PSAM channel estimation vs. the symbol-SNR when the angle spread is $\sigma_{AS} = 5^\circ$. Notice that AMREC of order $N = 2$ offers the lowest AEP when $E_b/N_0 < 8$ dB. For an AEP of 10^{-2} this choice of AMREC is about 0.9 dB better than MRCO, and about 4.2 dB better than Max-ASNR BF. Thus, a well-tuned MREC antenna system may yield important gains over a beamforming or an MRC antenna system, for small-to-moderate angle spreads. For higher SNR, AMREC of order $N = 3$ offers the minimum AEP. This suggests that for higher symbol-SNR, higher-order AMREC should be employed, although this results in a smaller complexity- and AEP-advantage of MREC over AMRCO. Again, the new criterion is shown to select the AMREC order which offers the lowest AEP and complexity.

In Fig. 7 we show the performance of EMREC and EMRCO with MMSE PSAM channel estimation vs. the symbol-SNR, E_b/N_0 when the angle spread is $\sigma_{AS} = 5^\circ$. The corresponding curves for SINC PSAM are similar but shifted downwards (not shown). Notice again that as the symbol-SNR increases, EMREC of higher order should be employed for minimum AEP.

The cause for the changes in the combiners' relative AEP-performance vs. symbol-SNR

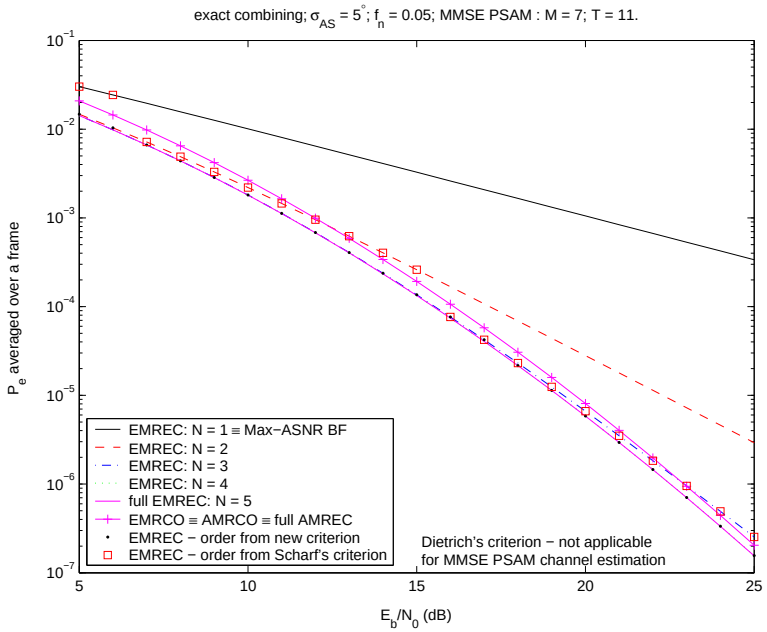

Fig. 7. AEP vs. the symbol SNR E_b/N_0, at $\sigma_{AS} = 5^\circ$, for exact combining and MMSE PSAM channel estimation; (30) is used for EMREC.

lies in their potential diversity gains given the branch correlation. Clearly, as the MREC order increases, the corresponding potential diversity gain is a larger share of the total available diversity gain, which is delivered by full MREC and MRCO. For any branch correlation, the slopes of the MREC/MRCO AEP-curves at high symbol-SNR reflect the potential diversity gain.

Fig. 8 presents the results obtained for two scattering regions, when the angle spread is $\sigma_{AS} = 5^\circ$. AMREC of order $N = 3$, selected based on the new criterion, yields an improvement of nearly 0.6 dB over AMRCO at $APE = 10^{-2}$.

C. The effect of fading rate on combining performance

In other results not shown here, the AEPs of exact and approximate MREC and MRCO were observed to be independent of the fading rate for SINC PSAM, which is as expected since a fixed interpolation filter is used in estimation. However, for MMSE PSAM, we noticed that faster fading may lead to significantly higher AEP. Nevertheless, SINC PSAM always leads to higher AEP than MMSE PSAM (much higher for slow fading). Furthermore, we noticed that MRCO and higher-order MREC improve faster than lower-order MREC when the fading rate is decreasing, which is also caused by the difference in their potential diversity

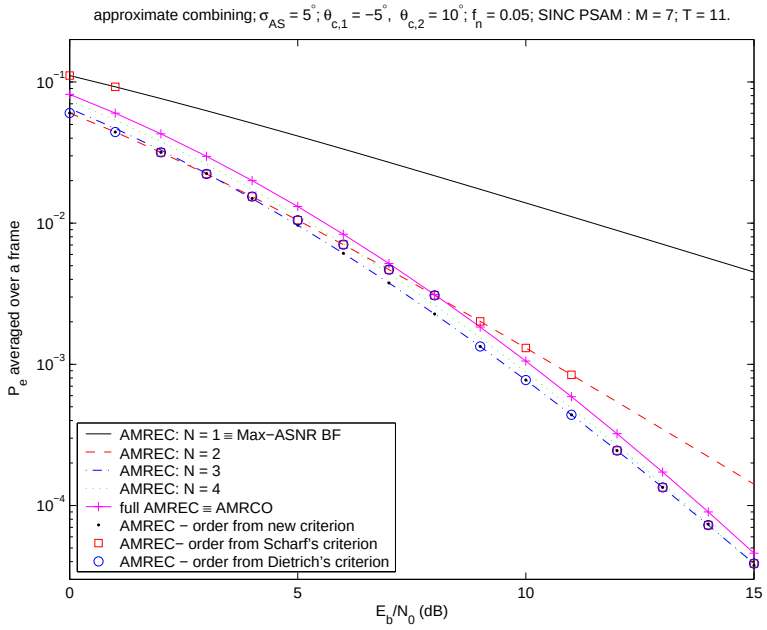

Fig. 8. AEP vs. the symbol SNR E_b/N_0, for approximate combining and SINC PSAM channel estimation, when 2 clusters of scatterers are present, one at $\theta_{c,1} = -5^\circ$, the other at $\theta_{c,2} = 10^\circ$, each with $\sigma_{AS} = 5^\circ$; (16) used for AMREC.

gains. This may also change the relative performance of the combiners, although not as significantly as when the symbol SNR is varied.

D. The effect of interpolator length on combining performance

The interpolator length T chosen for PSAM-based estimation (see Section II) directly impacts delay, computational load and detection performance [18]. Fig. 9 shows the behavior of MREC and MRCO for exact combining and MMSE PSAM vs. T. For $T = 1$ the processing is delay-free but yields high AEP. However, T (thus, the delay) does not have to be very large in order for the combining method to reach the full potential. Furthermore, the detection performance of higher-order MREC and of MRCO improves more quickly with increasing T, which may also lead to changes in the relative performance of these combiners.

VII. CONCLUSIONS

In this work, for MPSK modulation and Rayleigh fading, we provide an analytical study of maximal-ratio eigen-combining (MREC) and we compare it to maximum average signal-to-noise ratio beamforming (Max-ASNR BF) and maximal-ratio combining of the original untransformed received signals (MRCO), for antenna array systems. For imperfectly-known

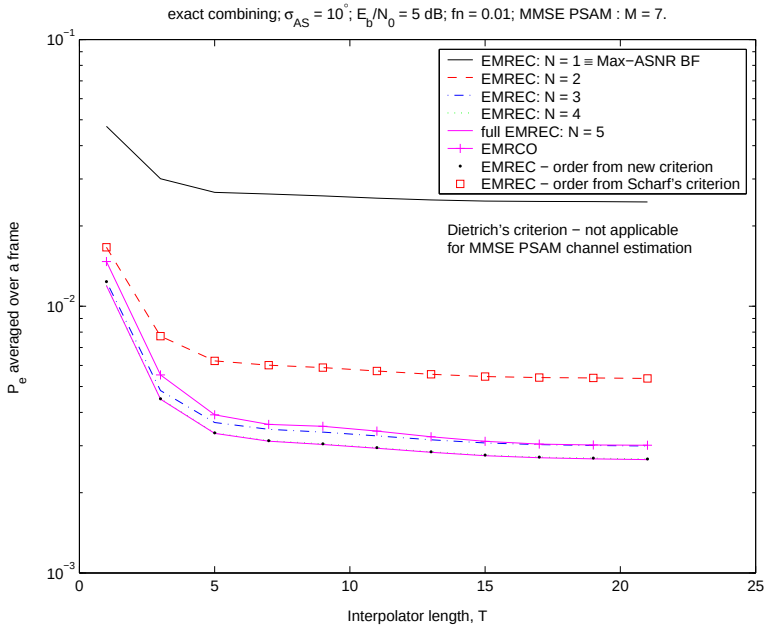

Fig. 9. AEP vs. the interpolator length T, at $\sigma_{AS} = 10^{\circ}$, for exact combining and MMSE PSAM channel estimation; (30) is used for EMREC.

correlated channels, we obtain average error probability (AEP) expressions for exact and approximate MREC, which may also be applied to Max-ASNR BF and MRCO. We also analyze specific channel estimation methods based on pilot-symbol-aided modulation and interpolation. For the adaptive tuning of MREC we propose a new criterion which accounts for the channel estimation accuracy and can trade-off detection performance and complexity in a smart antenna array system. Our numerical results show that MREC of order selected using the proposed method provides substantial gains over Max-ASNR BF as well as over MRCO in scenarios with high correlation among the received signals. Future work will attempt an analysis of the eigen-combining approach in the presence of interference.

REFERENCES

[1] J.-A. Tsai, M. Buehrer, and B. Woerner, "The impact of AOA energy distribution on the spatial fading correlation of linear antenna array," *Proceedings of the* 58*th IEEE Vehicular Technology Conference, VTC Spring'02*, vol. 2, pp. 933–937, May 2002.

[2] A. Kuchar, M. Tangemann, and E. Bonek, "A real-time DOA-based smart antenna processor," *IEEE Transactions on Vehicular Technology*, vol. 51, no. 6, pp. 1279–1293, Nov. 2002.

[3] J. S. Hammerschmidt, C. Brunner, and C. Drewes, "Eigenbeamforming — a novel concept in array signal processing," in *Proceedings of the European Wireless Conference 2000*, Dresden, Germany, Sept. 2000.

[4] D. G. Brennan, "Linear diversity combining techniques," *Proceedings of the IEEE*, vol. 91, pp. 331–356, Feb. 2003.

[5] R. A. Monzingo and T. W. Miller, *Introduction to Adaptive Arrays*. New York, NY: John Wiley, 1980.

[6] C. Brunner, W. Utschick, and J. A. Nossek, "Exploiting the short-term and long-term channel properties in space and time: eigenbeamforming concepts for the BS in WCDMA," *European Transactions on Telecommunications. Special Issue on Smart Antennas*, vol. 12, no. 5, pp. 365–378, 2001.

[7] J. Choi and S. Choi, "Diversity gain for CDMA systems equipped with antenna arrays," *IEEE Transactions on Vehicular Technology*, vol. 52, no. 3, pp. 720–725, May 2003.

[8] M. Kim, W.-C. Lee, J. Choi, and S. Choi, "Adaptive beamforming technique based on eigen-space method for a smart antenna in IS2000 1X environment," in *IEEE Antennas and Propagation Society International Symposium*, vol. 1, 2002, pp. 118–121.

[9] F. A. Dietrich and W. Utschick, "Maximum ratio combining of correlated Rayleigh fading channels with imperfect channel knowledge," *IEEE Communications Letters*, vol. 7, no. 9, pp. 419–421, Sept. 2003.

[10] F. Dietrich and W. Utschick, "On effective spatio-temporal rank of wireless communication channels," in *Proceedings of the 13th IEEE International Symposium on Personal, Indoor and Mobile Radio Communications, 2002*, vol. 5, Sept. 2002, pp. 1982–1986.

[11] R. A. Haddad and T. W. Parsons, *Digital signal processing: theory, applications, and hardware*. New York, NY: Computer Science Press, an imprint of W. H. Freeman and Co., 1991.

[12] X. Dong and N. Beaulieu, "Optimal maximal ratio combining with correlated diversity branches," *IEEE Communications Letters*, vol. 6, no. 1, pp. 22–24, Jan. 2002.

[13] J. Hammerschmidt and C. Brunner, "Merging diversity and beamforming perceptions in spatial signal processing," *Frequenz*, no. 5/6, May/June 2001.

[14] P. Polydorou and P. Ho, "Error performance of MPSK with diversity combining in non-uniform Rayleigh fading and non-ideal channel estimation," in *Proceedings of the* 51*st IEEE Vehicular Technology Conference, VTC Spring'00*, vol. 1, Tokyo, May 2000, pp. 627–631.

[15] J. Proakis, *Digital Communications*, 4th ed. Boston, MA: McGraw-Hill, 2001.

[16] P. Bello and B. D. Nelin, "Predetection diversity combining with selectively fading channels," *IRE Transactions on Communications Systems*, vol. 10, no. 1, pp. 32–42, Mar. 1962.

[17] B. R. Tomiuk, "Effects of imperfect maximal ratio combining on digital communications," Ph.D. dissertation, Queen's University, Kingston, ON, Canada, September 2002.

[18] J. K. Cavers, "An analysis of pilot symbol assisted modulation for Rayleigh fading channels," *IEEE Transactions on Vehicular Technology*, vol. 40, no. 4, pp. 686–693, Nov. 1991.

[19] W. C. Jakes, Ed., *Microwave mobile communications*. New York: John Wiley and Sons, 1974.

[20] N. W. K. Lo, D. D. Falconer, and A. U. H. Sheikh, "Adaptive equalization and diversity combining for mobile radio using interpolated channel estimates," *IEEE Transactions on Vehicular Technology*, vol. 40, no. 3, pp. 636–645, Aug. 1991.

[21] P. Shamain and L. B. Milstein, "Effect of mutual coupling and correlated fading on receive diversity systems using compact antenna arrays and noisy channel estimates," in *Proc. IEEE Global Telecommunications Conference, Globecom'03*, San Francisco, CA, Dec. 2003.

[22] I. S. Gradshteyn and I. M. Ryzhik, Eds., *Tables of integrals, series and products*, 4th ed. New York, NY: Academic Press, 1965.

[23] S. V. Amari and R. B. Misra, "Closed-form expressions for distribution of sum of exponential random variables," *IEEE Transactions on Reliability*, vol. 46, no. 4, pp. 519–522, Dec. 1997.

[24] M. K. Simon and M.-S. Alouini, *Digital communication over fading channels : a unified approach to performance analysis*. New York, NY: John Wiley and Sons, 2000.

[25] W. C. Y. Lee, *Mobile Communications Engineering*. New York, NY: McGraw-Hill, 1982.

[26] A. Naguib, "Adaptive antennas for CDMA wireless networks," Ph.D. dissertation, Stanford University, Stanford, CA, Aug. 1996.

[27] J. Jelitto and G. Fettweis, "Reduced dimension space-time processing for multi-antenna wireless systems," *IEEE Wireless Communications*, vol. 9, no. 6, pp. 18–25, Dec. 2002.

[28] L. L. Scharf, *Statistical Signal Processing. Detection, Estimation and Time Series Analysis*. Reading, MA: Addison-Wesley Publishing Company, 1991.